Sandia National Laboratories

NNM Force Appropriation Pre-test Prediction of Assembly using Calibrated Component and Modal Shaker Models

N-O-MAD Research Institute

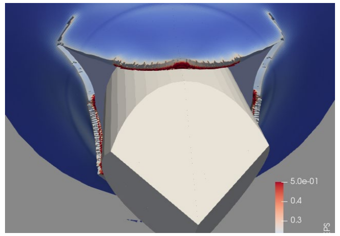

Students:

Arun Malla, Eric Robbins, and Trent Schreiber

Mentors:

Benjamin Pacini, Robert Kuether, Daniel Roettgen,

Simone Manzato, and Fernando Moreu

SAND2020-7662 PE

U.S. Department of Energy · NNSA National Nuclear Security Administration

Sandia National Laboratories is a multimission laboratory managed and operated by National Technology & Engineering Solutions of Sandia, LLC, a wholly owned subsidiary of Honeywell International Inc., for the U.S. Department of Energy's National Nuclear Security Administration under contract DE-NA0003525.

Content slide

I. Introduction

Background and Motivation

- Despite its effect on multiple aspects of structural dynamics, nonlinearity is under-considered and often neglected in industrial design and qualification
- To develop understanding of nonlinear structural dynamics, Seimens Industry Software attempted system identification on a demo aluminum aircraft (Fig. 1) [1]
- But, dynamics of the full system (wing+pylon+fixture) were too complex

Solution: Begin with isolated fixture-pylon structure

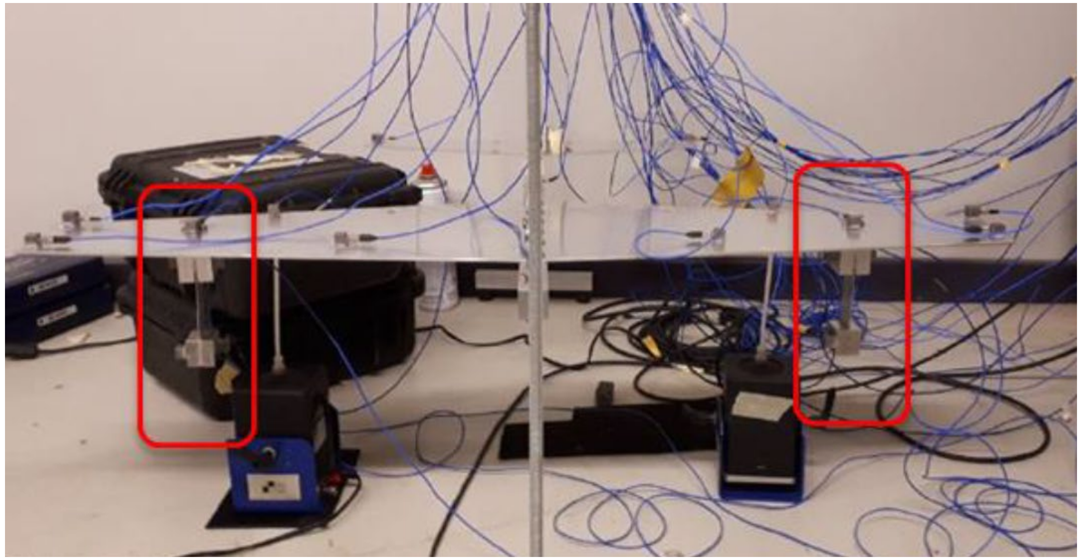

Fig. 1: Siemens demo aluminum aircraft [1]

Previous NOMAD Work

- A NOMAD 2019 research group studied the isolated fixture-pylon structure [2]
- Experiments were conducted on the setup shown in Fig. 2
  - Shaker was used to excite fixture-pylon structure
  - Data collected through accelerometers

Results:

Experimental data

Basic nonlinear model

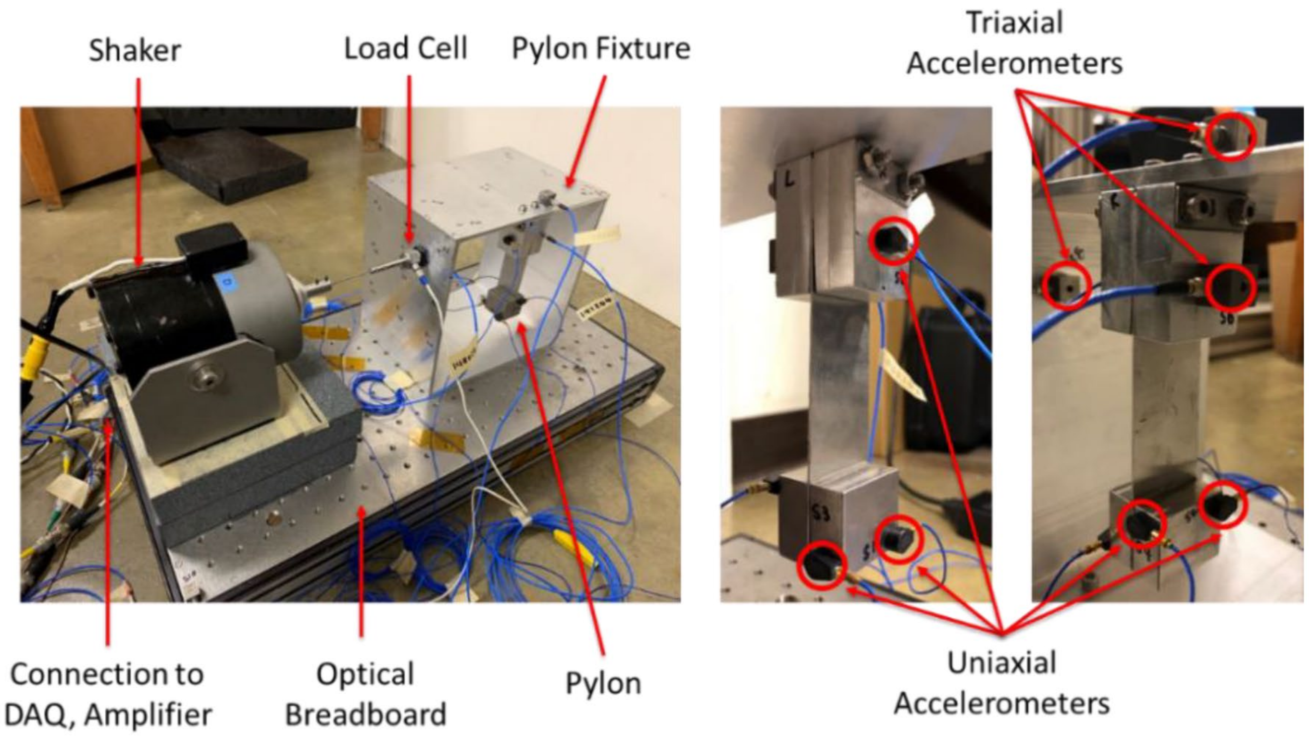

Fig. 2: Sandia isolated fixture-pylon test setup

Current Work

The NOMAD 2020 project builds upon the previous results by:

- Analyzing experimental data
- Further developing the nonlinear model of the fixture-pylon assembly
- Calibrating fixture-pylon model against experimental data
- Combining fixture-pylon model with linear model of the wing structure
- Analyzing the fixture-pylon and wing-pylon-fixture models
- Simulating experiments by coupling wing-pylon model to a shaker model

First step: Analyzing fixture-pylon experimental data

Experimental Data Analysis

Previous experiments resulted in sine spectra data from accelerometers

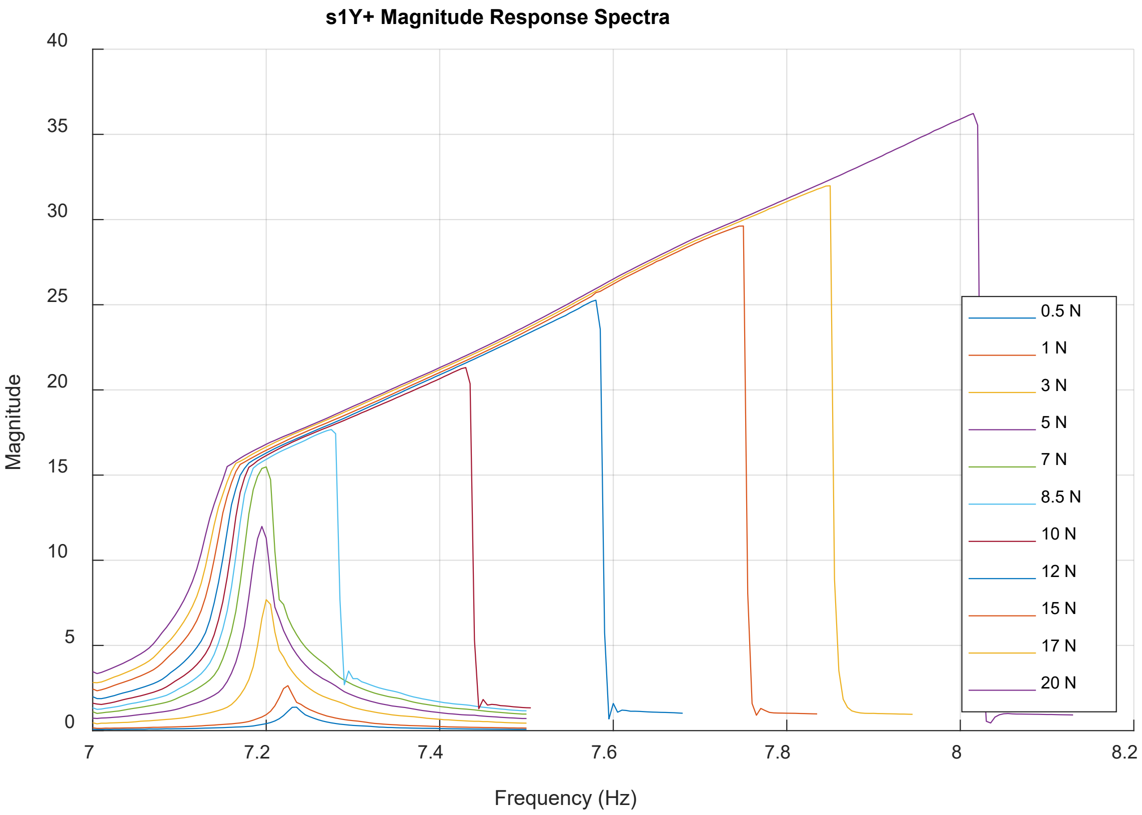

Fig. 3: Sine spectra magnitude response

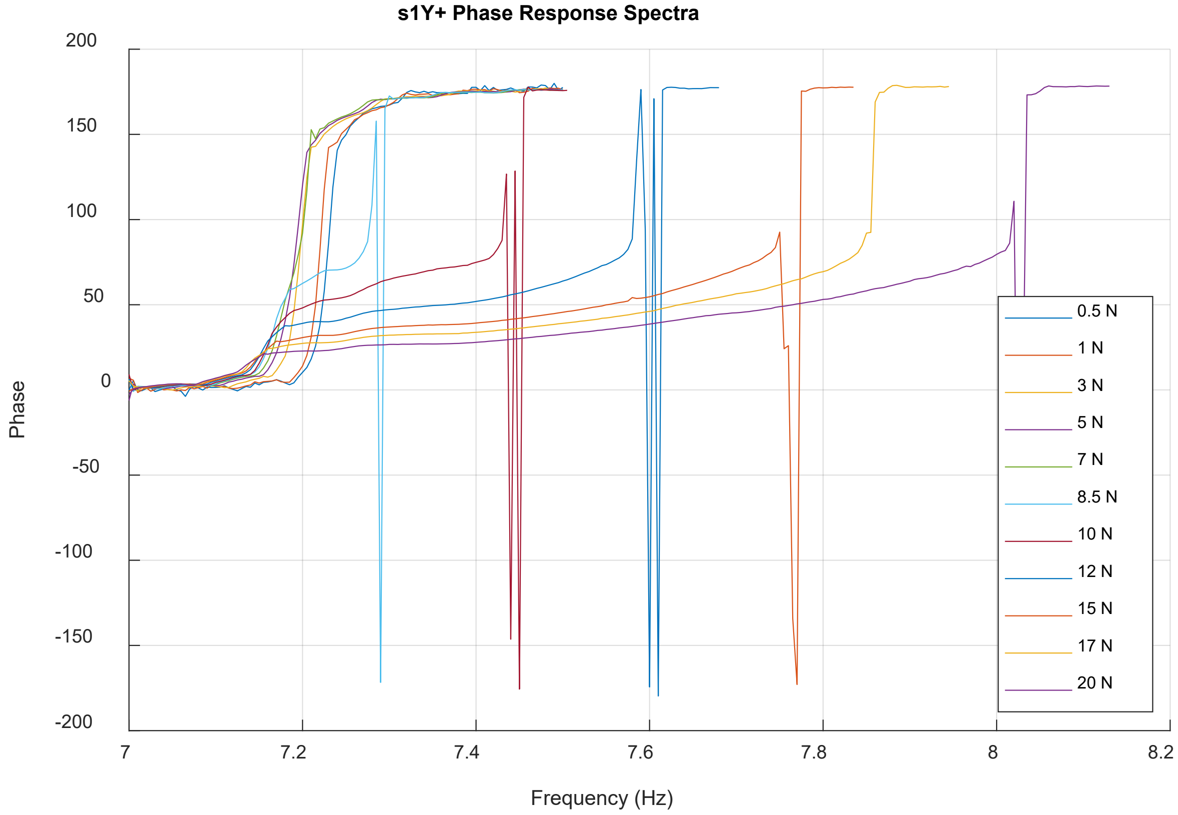

Fig. 4: Sine spectra phase response

Experimental Data Analysis (cont.)

From test data, we extracted backbone curves

- Backbone curves are a useful tool for understanding nonlinear behavior
- Backbone aligned with peaks of magnitude response

Backbone curves

=

Starting point

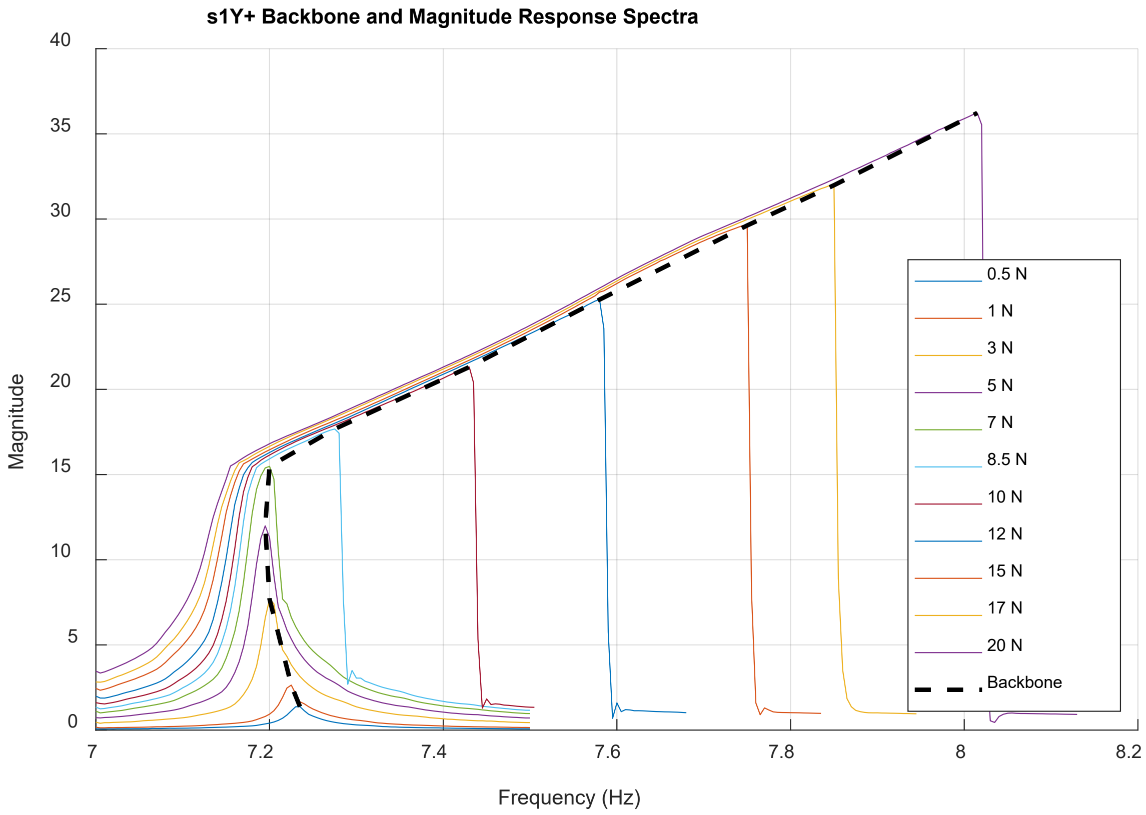

Fig. 5: s1Y+ backbone curve and magnitude response from sine spectra experimental data

II. Fixture-Pylon Assembly

Fixture-Pylon ROM

- To compare the experimental data to a numerical model, a linear finite element model was created for the fixture-pylon assembly using CUBIT
- To reduce the degrees of freedom (DOFs) in the model, a Craig-Bampton (CB) reduction was run in Sierra SD to obtain a reduced order model (ROM) [3-4]
  - This takes the full model with thousands of DOFs and reduces it to a more manageable model with only 7 retained DOFs (virtual nodes, accelerometers, and drive point)

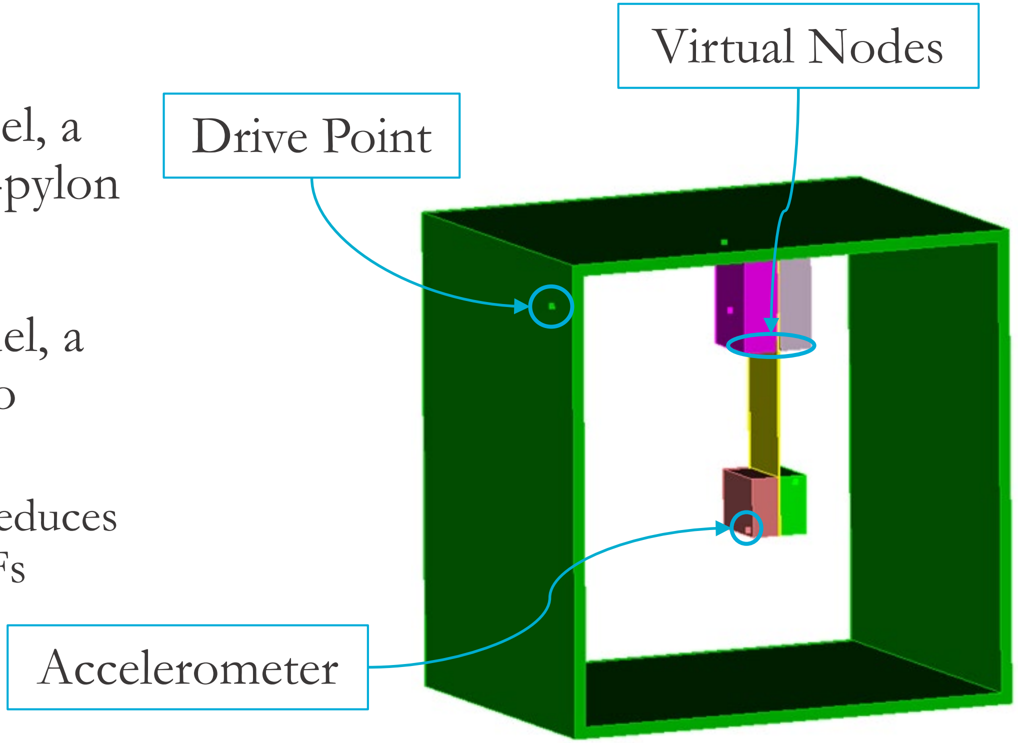

Fig. 6: Fixture-pylon CAD assembly

Reduce the full model to something more manageable:

Full model → CB reduction → Linear ROM

Fixture-Pylon ROM (cont.)

- The <u>linear</u> ROM from Sierra provides the mass and stiffness matrices for the fixture-pylon
  - Damping matrix is computed using proportional damping
- To convert the <u>linear</u> ROM to a <u>nonlinear</u> model, virtual nodes were tied to the pylon block so that a nonlinear restoring force could be added to the equations of motion (EOMs)
- EOMs of nonlinear dynamic system:

$$\underbrace{\boldsymbol{M}\ddot{\boldsymbol{x}}(\boldsymbol{t}) + \boldsymbol{C}\dot{\boldsymbol{x}}(\boldsymbol{t}) + \boldsymbol{K}\boldsymbol{x}(\boldsymbol{t})}_{\text{Linear ROM (Sierra Output)}} + \boxed{\boldsymbol{f}_{\boldsymbol{nl}}\{\boldsymbol{x}(\boldsymbol{t})\}} = \boldsymbol{u}$$

Nonlinear restoring force between virtual nodes (MATLAB)

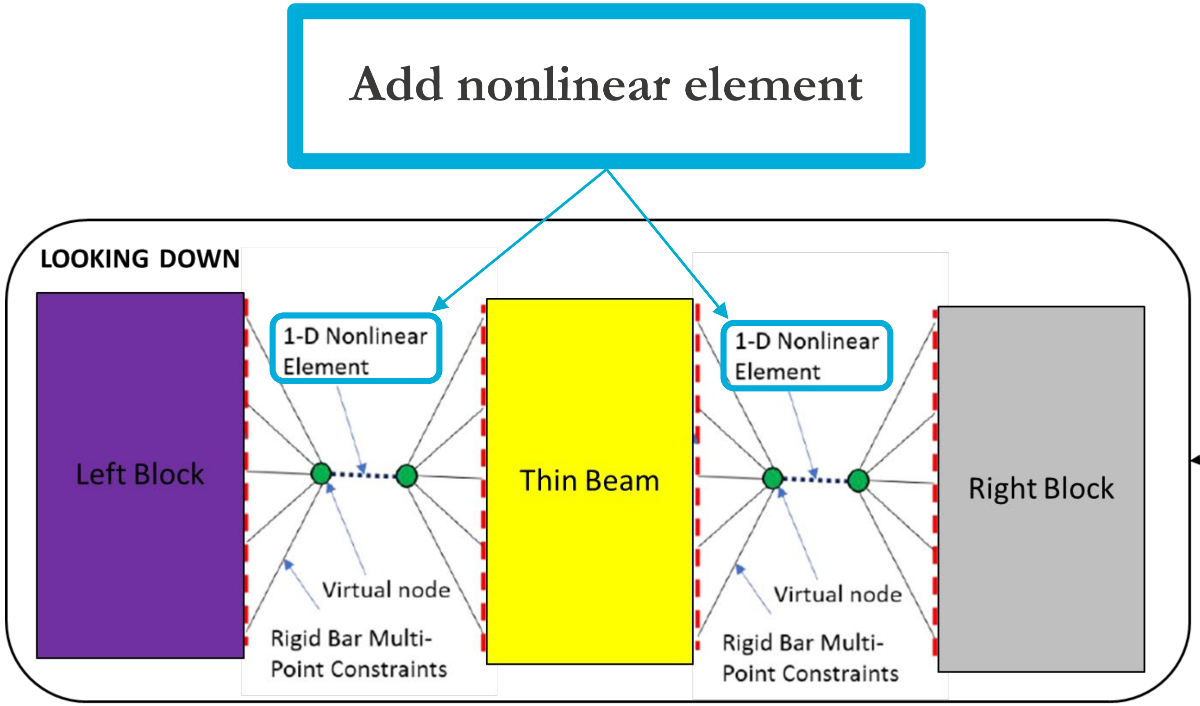

Fig. 7: Virtual nodes in pylon block

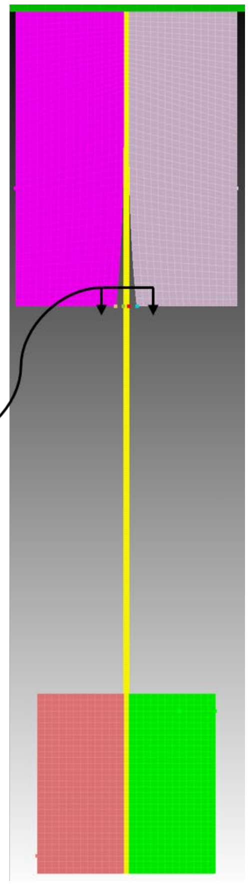

Nonlinear Normal Mode (NNM) Theory

- For an unforced, undamped system, an NNM is defined as a **response that is periodic but not necessarily synchronous** [5-6]
- A multi-degree of freedom system will have multiple NNMs
- NNMs are often illustrated in a frequency - energy plot (FEP) (Fig. 8), which shows how a system's natural frequency changes with energy input into the system
- Each point along the NNM in the FEP corresponds to a different time-history response
- Multi-harmonic balance (MHB) is one of several numerical methods used to compute NNMs

NNMs are computed using MHB and illustrated in frequency - energy plots

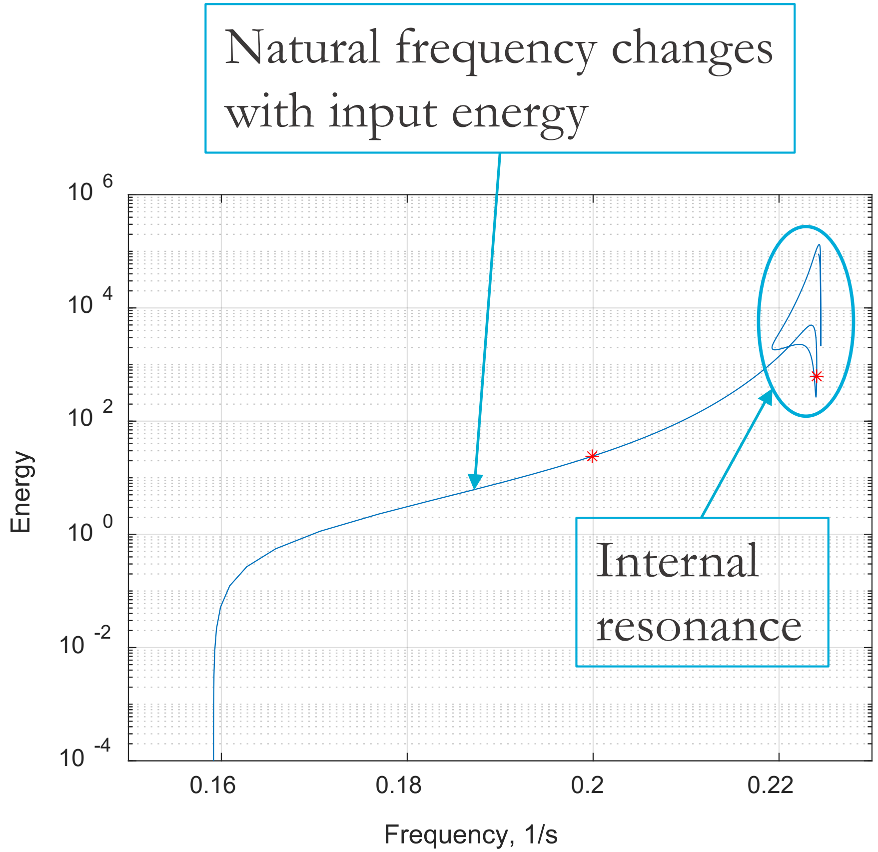

Fig. 8: Frequency - energy curve for 1st NNM of sample system

Calibrating ROM Nonlinearity

Two options were considered for nonlinear elements:

- Cubic spring element (Fig. 9)
  - $f_{\mathrm{nl}}(\Delta x) = k_{NL}(\Delta x)^3$
  - Parameters:
    - k_{NL}- nonlinear spring constant

- Gap-spring element (Fig. 10)
  - $f_{nl}(\Delta x) = \begin{cases} 0 \; for \; \Delta x \leq x_{gap} \\ k_{pen}(\Delta x - x_{gap}) \; for \; \Delta x > x_{gap} \end{cases}$
  - Parameters:
    - k_{pen}- linear penalty spring constant
    - x_{gap}- gap width

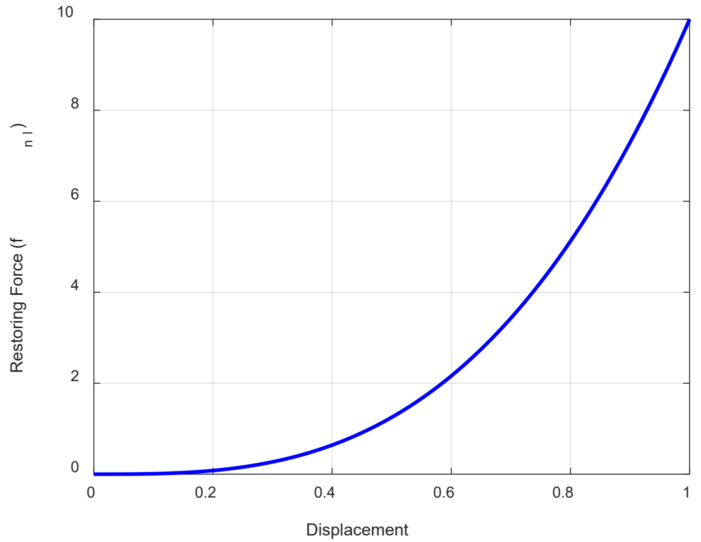

Fig. 9: f_{nl} for cubic spring element

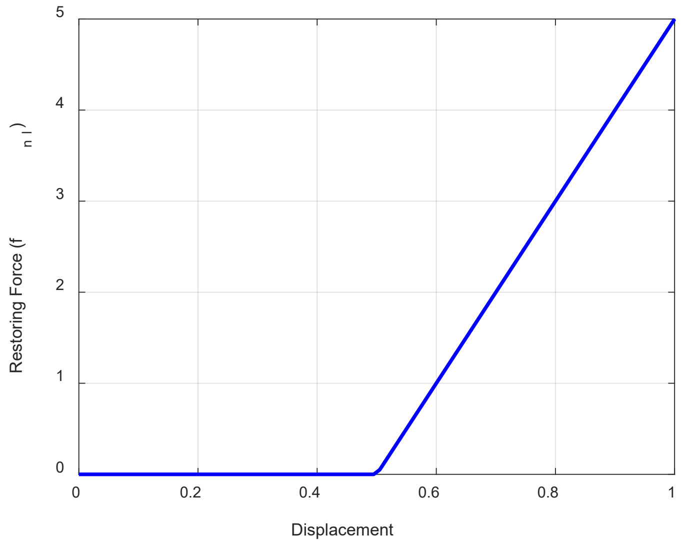

Fig. 10: f_{nl} for gap-spring element

Calibrating ROM Nonlinearity (cont.)

With cubic spring (Fig. 11) and gap-spring (Fig. 12) elements, NNM backbone curves were determined and compared to experimental data

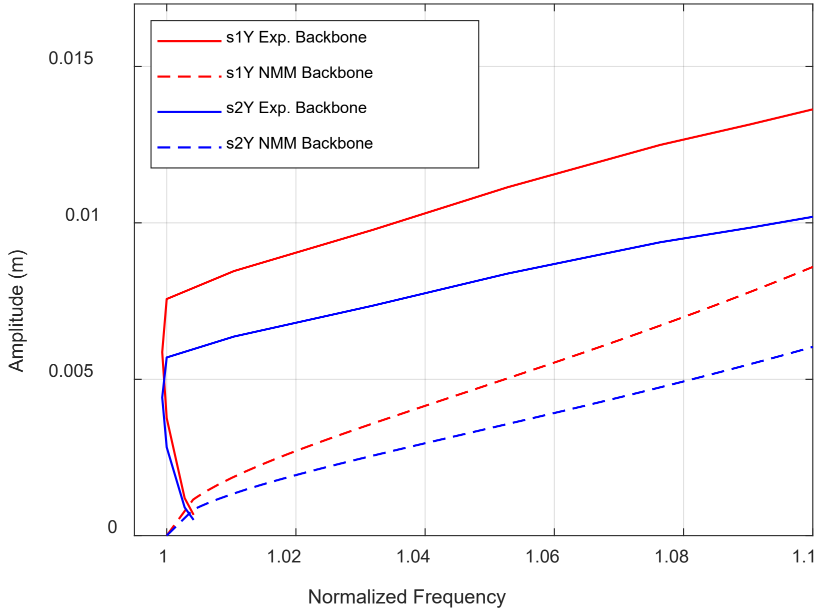

Fig. 11: Cubic spring element backbone comparison

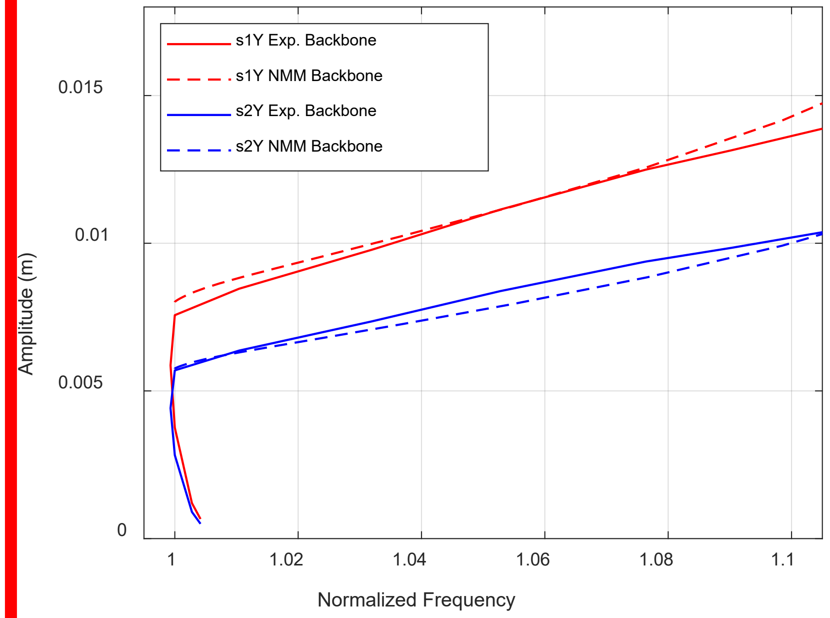

Fig. 12: Gap-spring element backbone comparison

Selected:

Gap-spring element

$$k_{pen} = \mathbf{7 * 10\text{^}4}\ N/m$$

$$x_{gap} = \mathbf{0.68}\ mm$$

Stepped Sine Validation

A stepped sine test simulation was performed to verify that the gap-spring nonlinearity accurately captures the nonlinear dynamics in the pylon-fixture ROM in comparison to the NOMAD 2019 experimental results

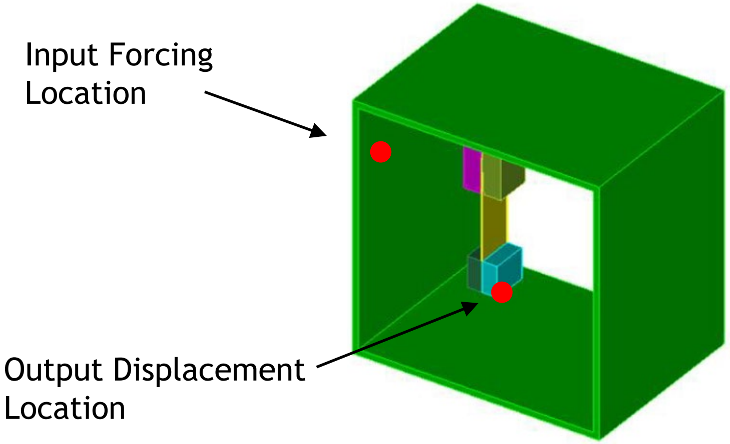

Fig. 13: Fixture-pylon system with marked input and output nodes

A stepped sine test simulation will verify if the calibrated ROM is in agreement with the experimental data

Stepped Sine Validation (cont.)

- Despite some variation in stiffness effects, the simulation results compared relatively well with the experimental results
- Nearly all linear-peak regions occurred at a slightly higher frequency and most nonlinear-peaks were slightly smaller in magnitude, compared to the experimental results

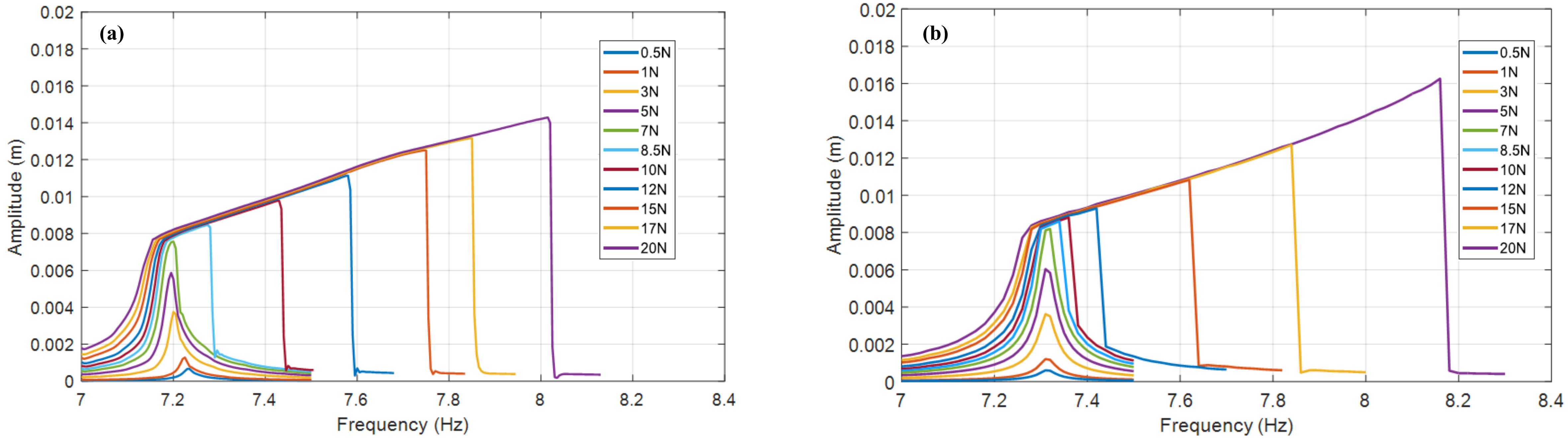

Fig. 14: Comparison of results from NOMAD 2019 experiment (a) and stepped sine simulation (b)

Stepped Sine Validation (cont.)

- Despite some variation in stiffness effects, the simulation results compared relatively well with the experimental results
- Nearly all linear-peak regions occurred at a slightly higher frequency and most nonlinear-peaks were slightly smaller in magnitude, compared to the experimental results

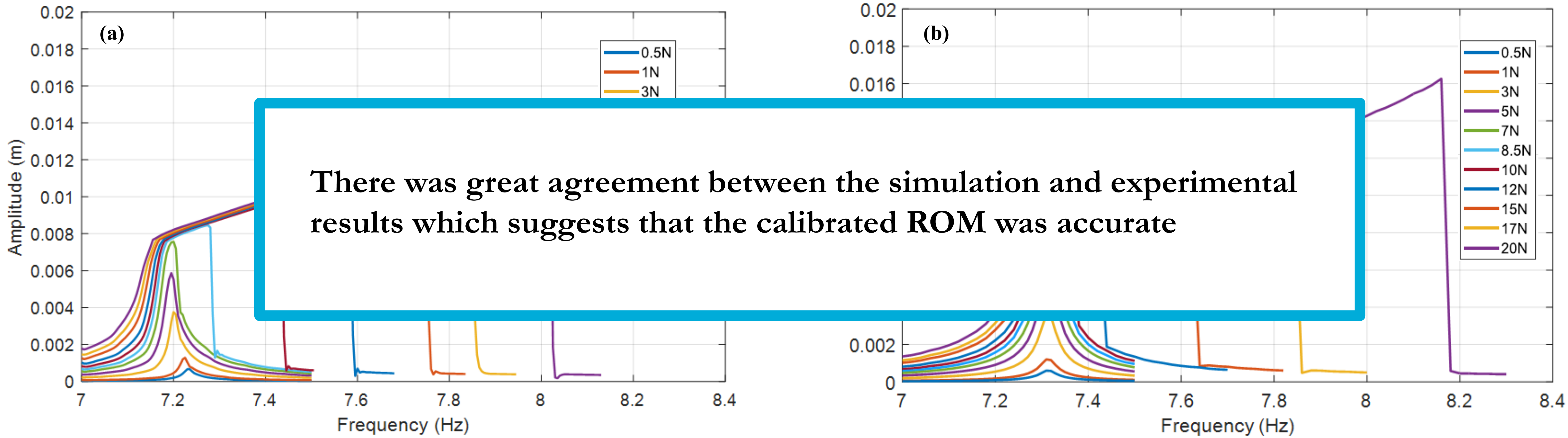

There was great agreement between the simulation and experimental results which suggests that the calibrated ROM was accurate

Fig. 14: Comparison of results from NOMAD 2019 experiment (a) and stepped sine simulation (b)

III. Full Assembly

Wing-Pylon ROM

- Next step: Attach the calibrated pylon to the wing
- Following similar methods as the fixture-pylon model, a linear finite element model of the next-level wing-pylon assembly was created
- Craig-Bampton reduction was applied using Sierra SD to obtain the linear ROM
  - DOFs for the accelerometers, virtual nodes, and drive points were retained
- The <u>calibrated</u> gap-spring element in the pylon block was added to the linear ROM to describe the nonlinear EOMs

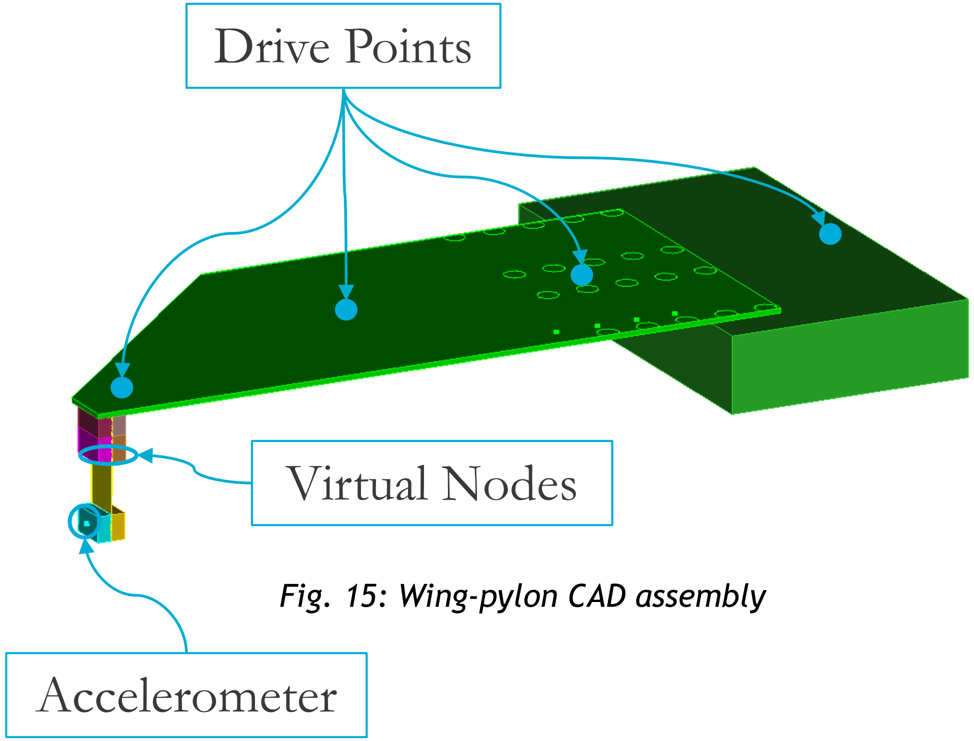

Fig. 15: Wing-pylon CAD assembly

Linear wing-pylon ROM from Sierra + **Calibrated gap-spring element in pylon** = **Nonlinear EOMs**

$$\boldsymbol{M\ddot{x}(t) + C\dot{x}(t) + Kx(t)} \qquad \boldsymbol{f_{nl}\{x(t)\}} \qquad \boldsymbol{M\ddot{x}(t) + C\dot{x}(t) + Kx(t) + f_{nl}\{x(t)\} = u}$$

Wing-Pylon ROM (cont.)

Mode shapes for linear wing-pylon model:

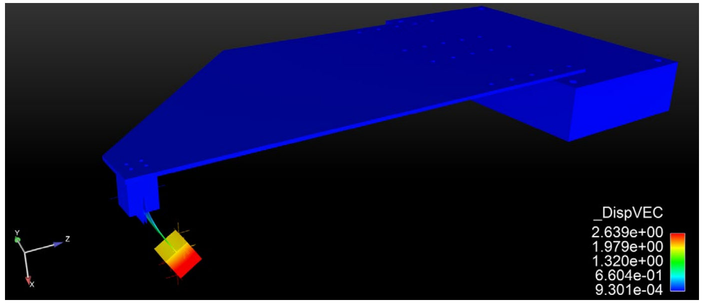

Fig. 16: Mode 1 (7.30 Hz)

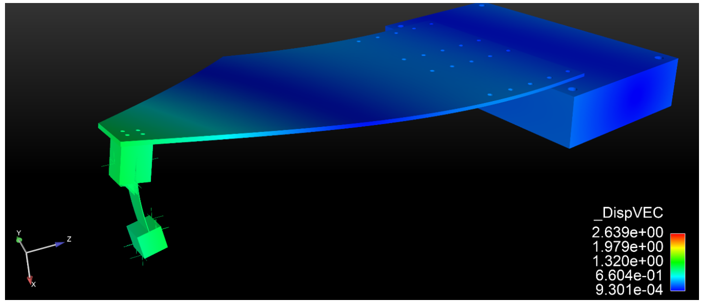

Fig. 17: Mode 2 (22.20 Hz)

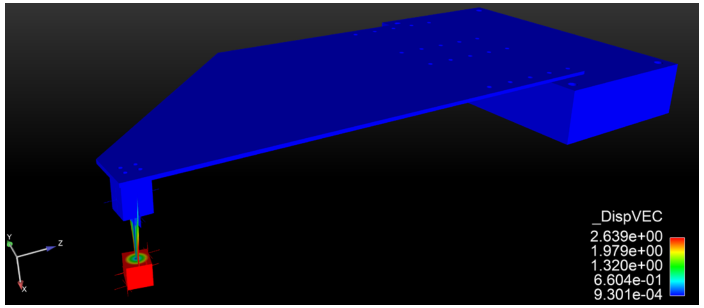

Fig. 18: Mode 3 (47.28 Hz)

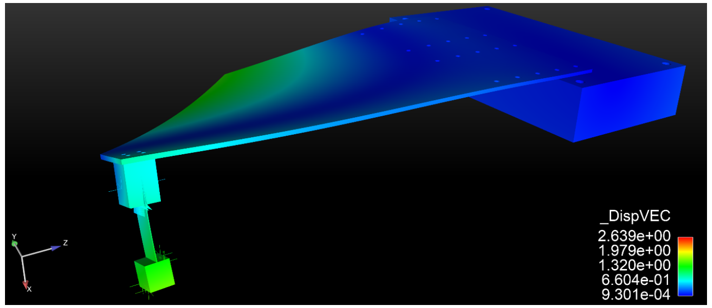

Fig. 19: Mode 4 (49.22 Hz)

Note: mode numbers refer to elastic modes

Multi-Harmonic Balance Method

- The MHB method was utilized to identify NNMs and any possible internal resonances for the calibrated wing-pylon ROM
- Mode 2 was of interest because the bending of the wing resulted in bending of the pylon beam which produced large displacements in the lower pylon block
- Large displacements in the pylon initiated the nonlinear behavior in the gap-spring element

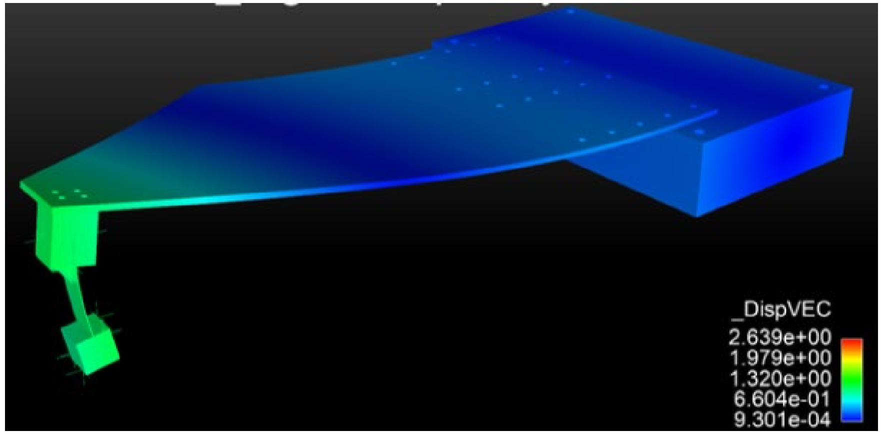

Fig. 20: Mode 2 (22.20 Hz)

Mode 2 was considered for further investigation based on the large wing and pylon bending mode shapes

Multi-Harmonic Balance Method (cont.)

- NNM 2 contained a small frequency shift which remained extremely close to linear mode 2 resonant frequency
- This can easily be overlooked if only a linear analysis is considered thus reinforcing the significance of nonlinear analyses
- An internal resonance was identified on a tongue of NNM 2

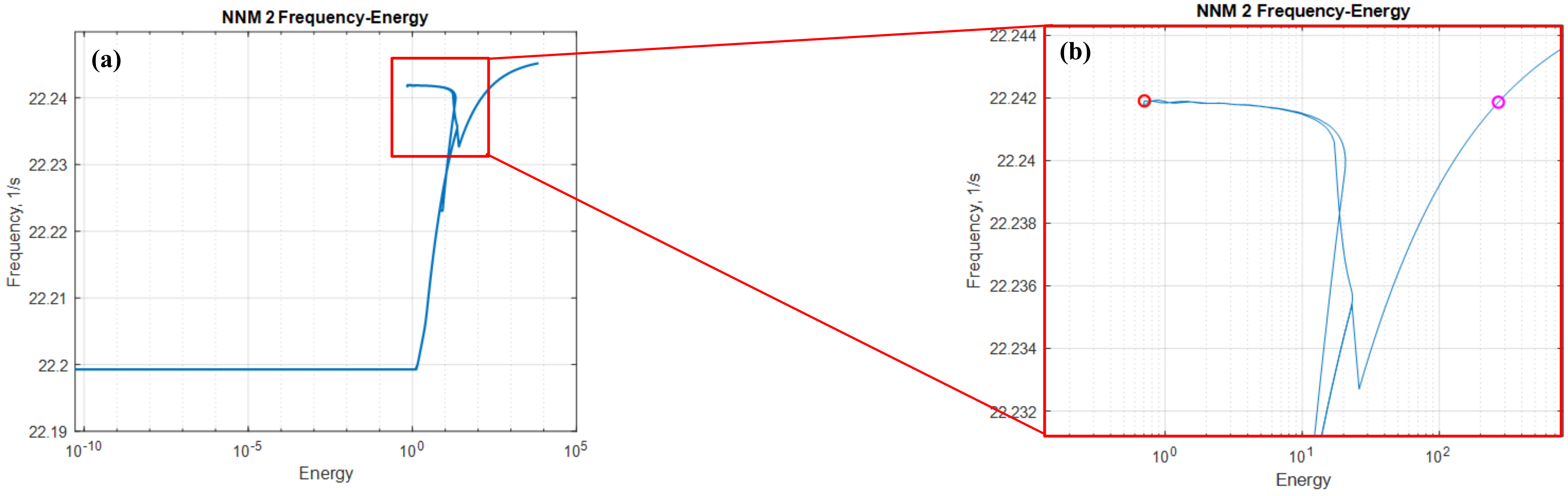

Fig. 21: NNM 2 of the Wing-Pylon Assembly

Fig. 22: NNM 2 with Identified Internal Resonance and Single Harmonic Points

Multi-Harmonic Balance Method (cont.)

- A 1:5 internal resonance was identified between NNM 2 and 7 on the wing-pylon ROM; the red point in (a) is the tongue of the internal resonance between the two NNM's
- The internal resonance can easily be seen in the displacement time-history (b) where multiple ratios of 1:5 harmonics exist
- Single harmonic motion exists (c) in NNM 2 as well which is described by the magenta point in (a)

NNM 2 remained very close to its linear mode and additionally contained a 1:5 internal resonance with NNM 7

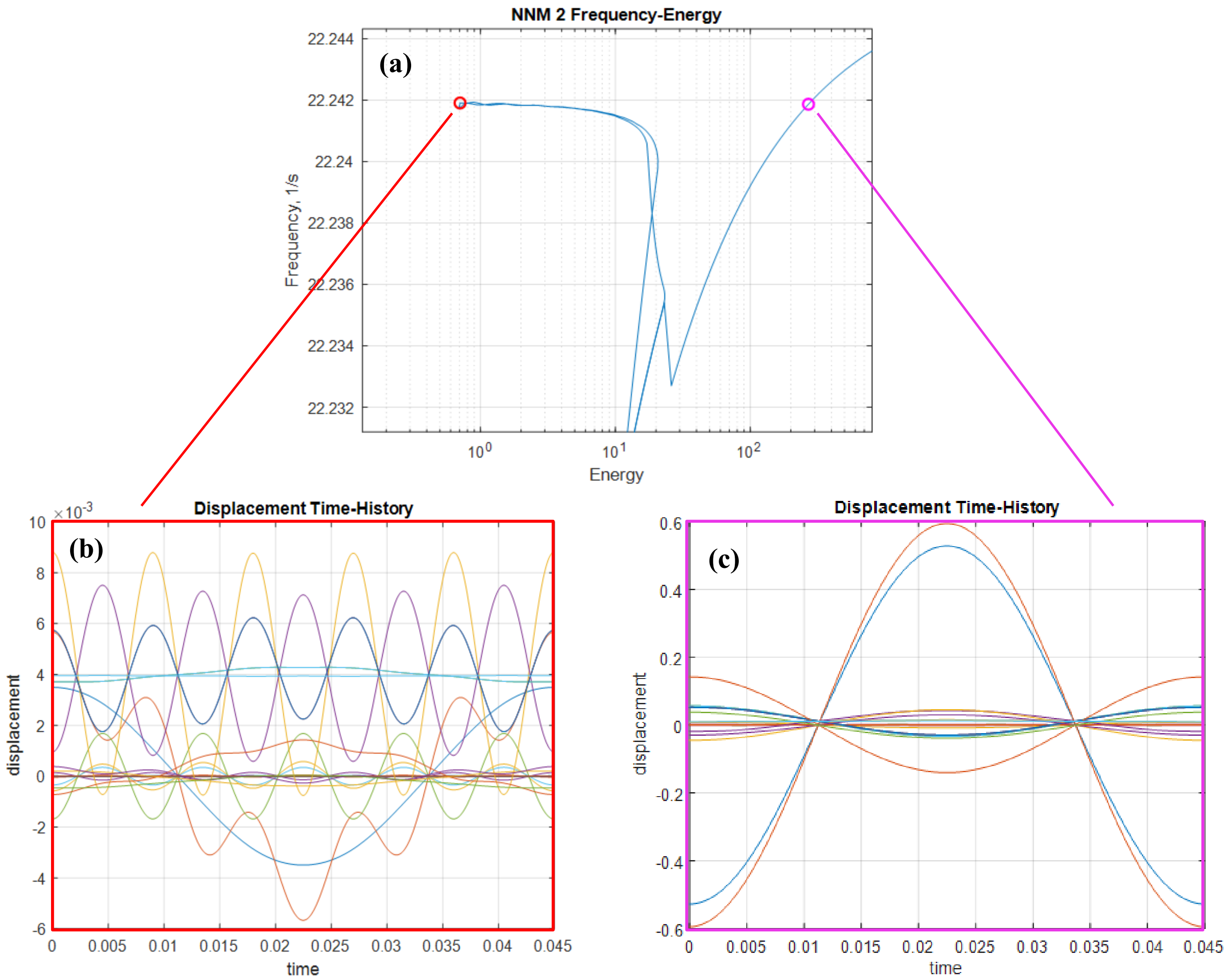

Fig. 23: Displacement Time-Hitories of Identified Internal Resonance and Single Harmonic Motion

Multi-Harmonic Balance Method (cont.)

- The modal interaction between the NNM's 2 and 7 are depicted in plot (b) where NNM 7 was scaled down by an integer of 5 and only computed to the 5th harmonic (there are more harmonics and internal resonances on NNM 7)
- This essentially means when mode 2 is excited mode 7 can experience large displacement amplitude responses

(a)

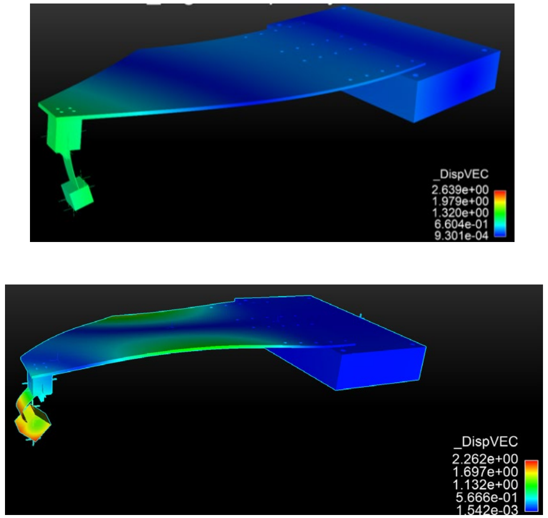

Fig. 24: Linear Modes 2 and 7 Mode Shapes

(b)

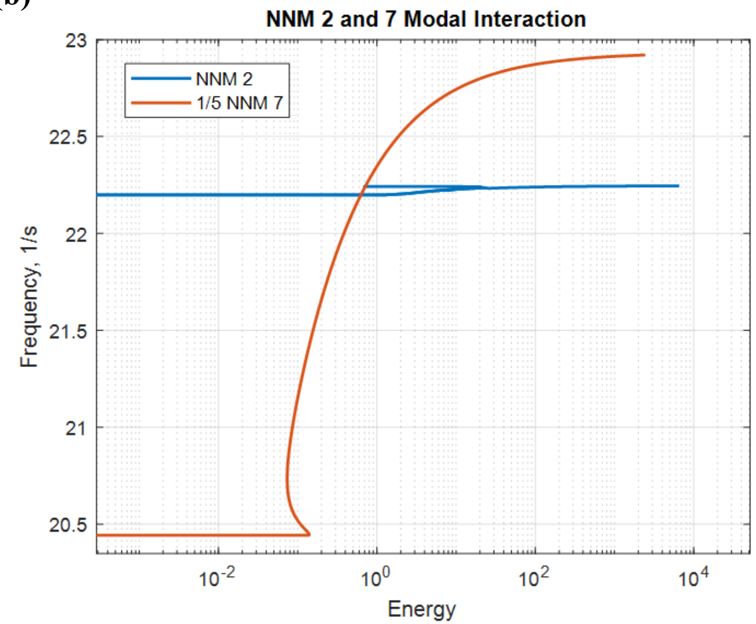

Fig. 25: NNM 2 and 7 Modal Interaction

(c)

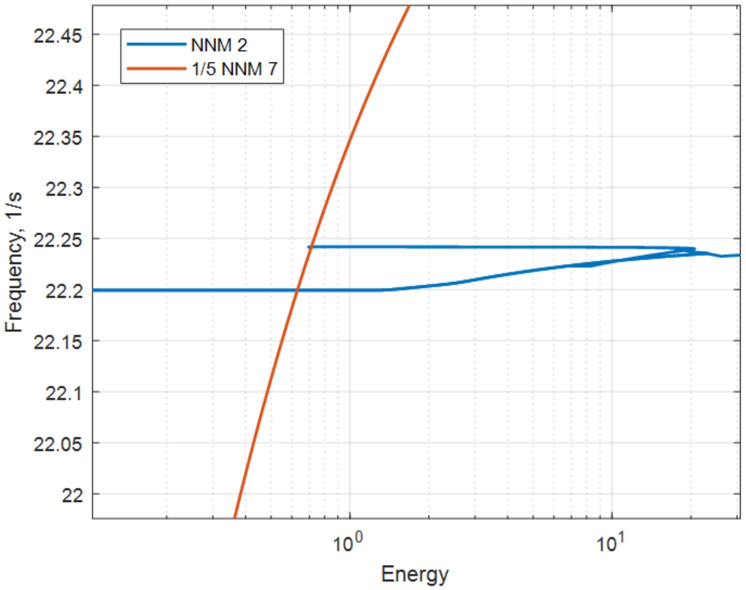

Fig. 26 NNM 2 and 7 Internal Resonance Crossing

Multi-Harmonic Balance Method (cont.)

- The modal interaction between the NNM's 2 and 7 are depicted in plot (b) where NNM 7 was scaled down by an integer of 5 and only computed to the 5th harmonic (there are more harmonics and internal resonances on NNM 7)
- This essentially means when mode 2 is excited mode 7 can experience large displacement amplitude responses

(a)

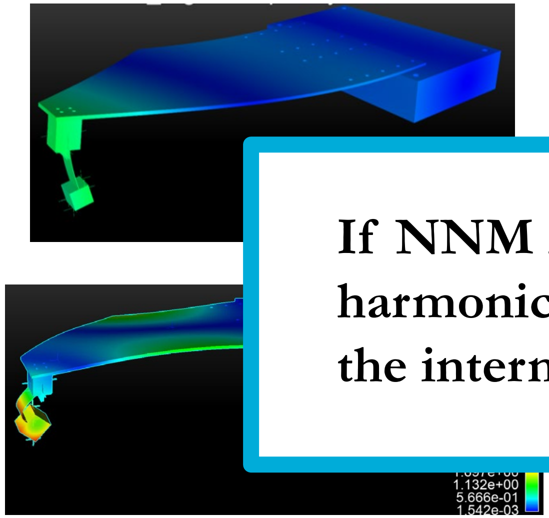

Fig. 24: Linear Modes 2 and 7 Mode Shapes

(b)

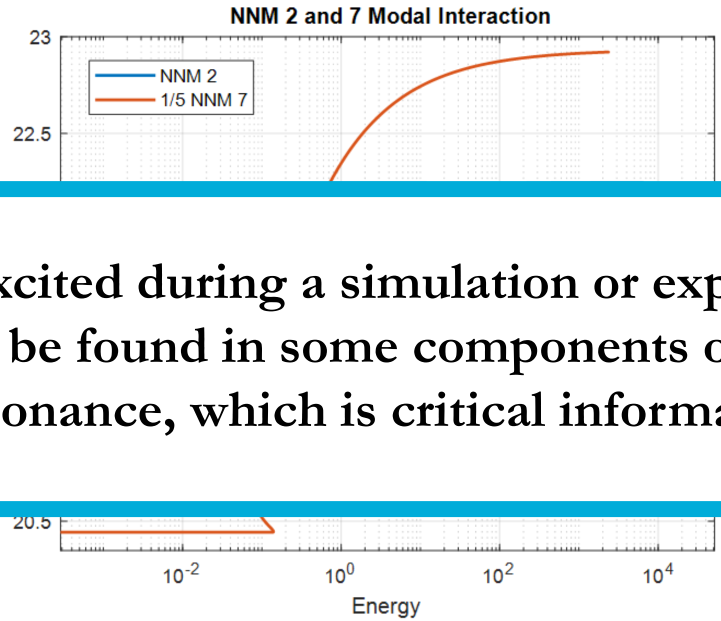

Fig. 25: NNM 2 and 7 Modal Interaction

(c)

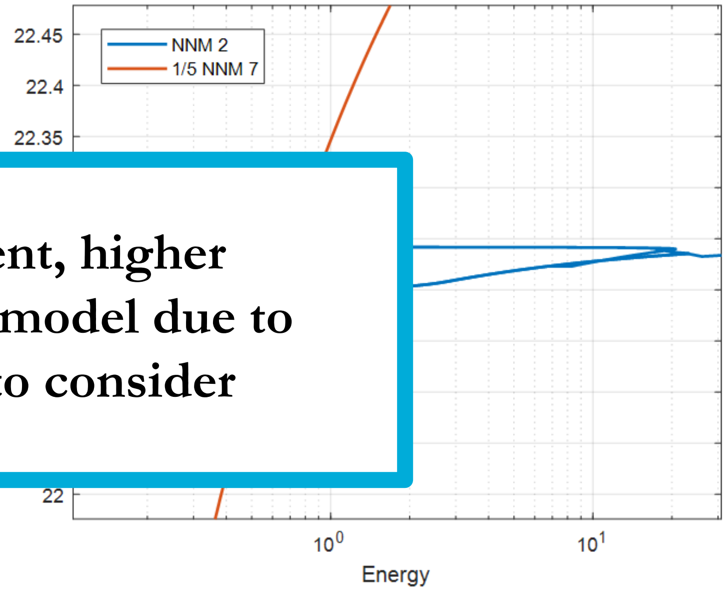

Fig. 26 NNM 2 and 7 Internal Resonance Crossing

If NNM 2 is excited during a simulation or experiment, higher harmonics can be found in some components of the model due to the internal resonance, which is critical information to consider

IV. Virtual Experiments

Shaker Model

To account for physical limitations of the shaker, a previously calibrated electro-mechanical shaker model was substructured to the wing-pylon ROM for simulated experiments using the force appropriation method

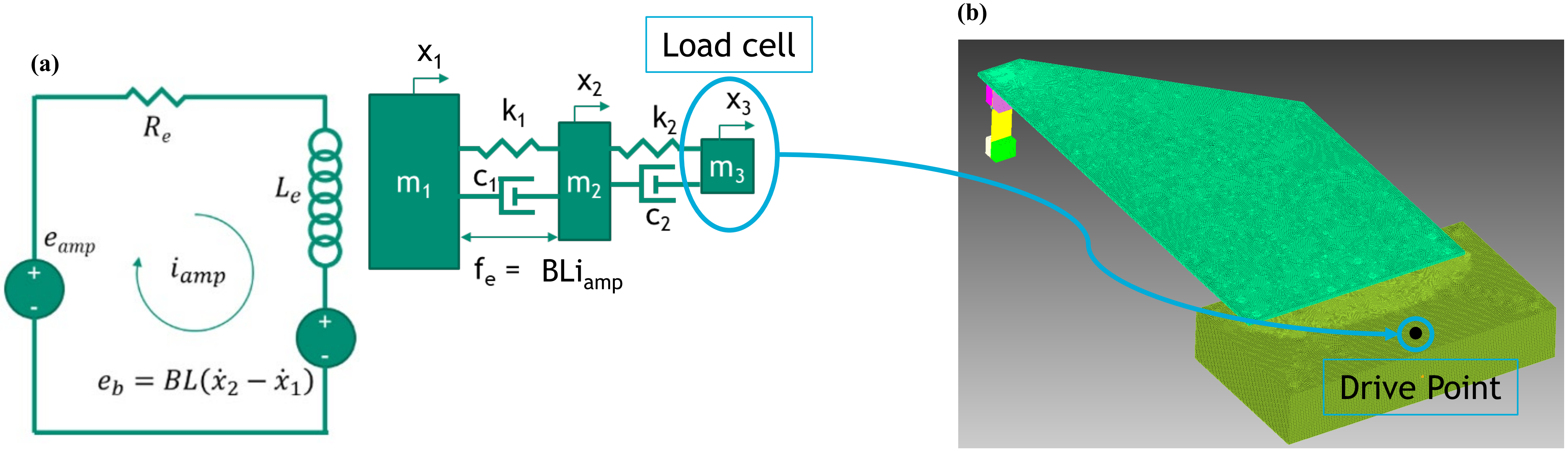

Fig. 27: Virtual shaker model (a) and wing-pylon finite element model (b)

Note: Shaker input voltage is the <u>only</u> input to the substructured shaker, wing, pylon system

Force Appropriation Method

- Phase lag quadrature criterion: A single NNM is isolated if the structure vibrates with a phase lag of 90° with respect to the input signal
- Force appropriation testing relies on the phase lag quadrature criterion
  - The structure is excited at different forcing frequencies until a 90° phase difference is achieved
  - NNMs can be identified one at a time using this method
- Simulated force appropriation experiments were performed for the wing-pylon assembly
  - A controller varied the <u>frequency</u> of the shaker input voltage until quadrature was achieved
  - The amplitude of the input voltage was then increased and the process repeated; thus constructing the frequency-energy plot (FEP) for NNMs of interest

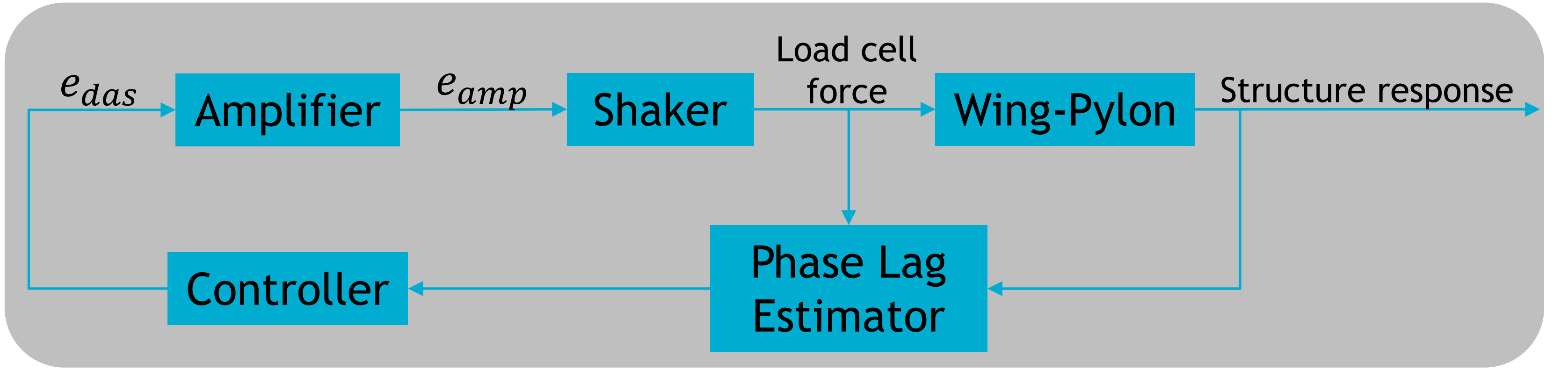

Fig. 28: Block diagram of force appropriation testing

Force Appropriation Method (cont.)

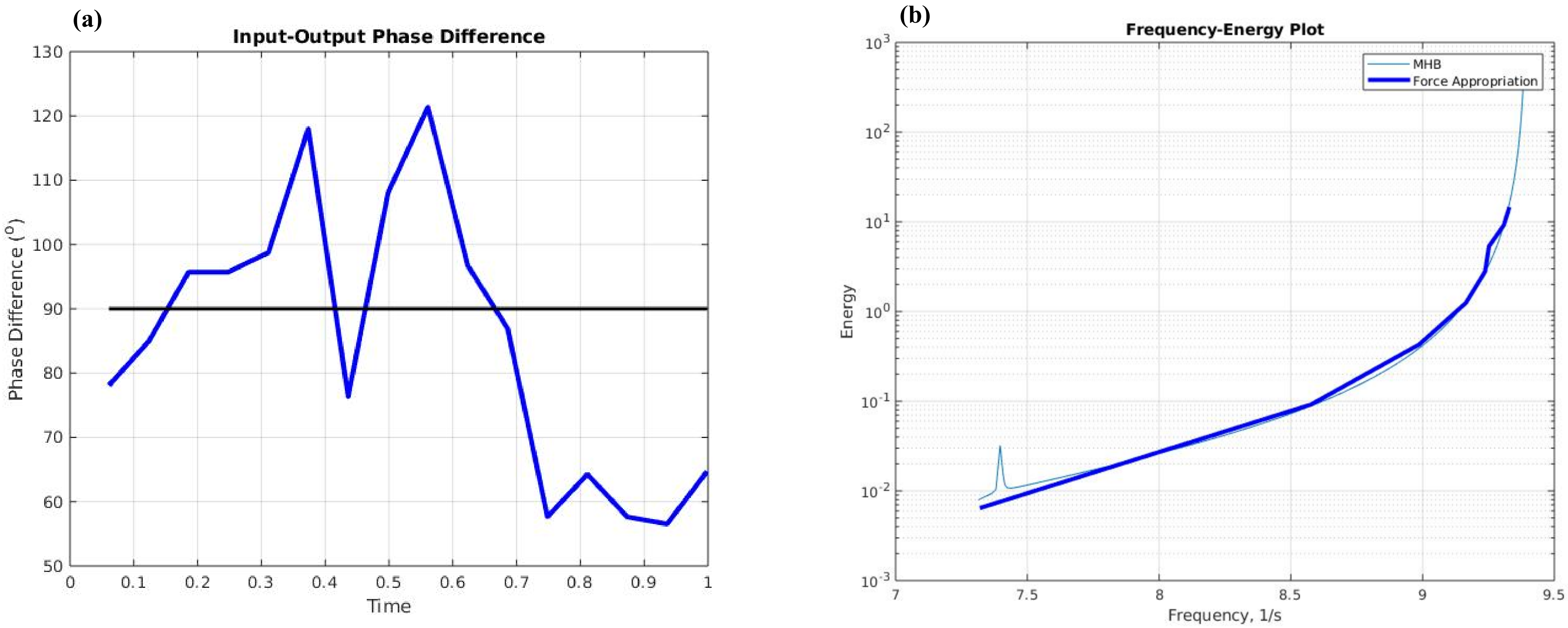

Fig. 29: NNM 1 phase lag quadrature quality (a) and FEP (b)

Further work needs to be conducted to achieve better quadrature

V. Conclusions

Results, Conclusions and Future Work

Results

- NNMs were successfully characterized using computational methods such as force appropriation and multi-harmonic balance
- Models were accurately validated against experimental data and finite element software
- It was shown that the study of NNMs can yield insights into nonlinear systems, such as the presence and behavior of internal resonances as well as the frequency-energy dependence of nonlinear modes
- To simulate a physical experiment, a calibrated shaker model was substructured to the wing-pylon model

Future Work:

- Fine-tune simulation model to accurately simulate second and higher modes
- Experimental testing of the physical wing-pylon assembly to validate NNMs and internal resonances between different combinations of modes
- Further investigations can be conducted on the effect of other system parameters such as wing length

THANK YOU

References

[1] Cooper, S.B., et al. *Investigating Nonlinearities in a Demo Aircraft Structure Under Sine Excitation*. 2020. Cham: Springer International Publishing.

[2] Ligeikis, C., et al., Modeling and Experimental Validation of a Pylon Subassembly Mockup with Multiple Nonlinearities, in 38th International Modal Analysis Conference (IMAC XXXVIII), 2020, Houston, TX.

[3] Craig, R.R.J. and M.C.C. Bampton, Coupling of Substructures for Dynamic Analysis. AIAA Journal, 1968. 6(7): p. 1313-1319.

[4] Craig, R.R.J. and A.J. Kurdila, Fundamentals of Structural Dynamics. 2nd ed. 2006, New York: John Wiley and Sons.

[5] Kerschen, G., et al., Nonlinear normal modes. Part I. A useful framework for the structural dynamicist. Mechanical Systems and Signal Processing, 2009.

[6] Haller, G., Ponsioen, S., Nonlinear normal modes and spectral submanifolds: Existence, uniqueness, and use in model reduction. Nonlinear Dynamics, 2016.

[7] T. Detroux, L. Renson, L. Masset, and G. Kerschen, "The harmonic balance method for bifurcation analysis of large-scale nonlinear mechanical systems," *Computer Methods in Applied Mechanics and Engineering*, vol. 296, pp. 18-38, 2015/11/01/ 2015, doi: https://doi.org/10.1016/j.cma.2015.07.017

Acknowledgements

This research was conducted at the 2020 Nonlinear Mechanics and Dynamics Research Institute hosted by Sandia National Laboratories and the University of New Mexico.

Sandia National Laboratories is a multimission laboratory managed and operated by National Technology and Engineering Solutions of Sandia, LLC., a wholly owned subsidiary of Honeywell International, Inc., for the U.S. Department of Energy's National Nuclear Security Administration under contract DE-NA-0003525.